

## Endoproteolytic Cleavage of FE65 Converts the Adaptor Protein to a Potent Suppressor of the sAPP $\alpha$ Pathway in Primates\*

Received for publication, October 19, 2004, and in revised form, December 23, 2004  
Published, JBC Papers in Press, January 12, 2005, DOI 10.1074/jbc.M411855200

Qubai Hu<sup>‡</sup>, Lin Wang, Zheng Yang, Bethany H. Cool, Galynn Zitnik, and George M. Martin

From the Department of Pathology, University of Washington, Seattle, Washington, 98195

**Adaptor protein FE65 (APBB1) specifically binds to the intracellular tail of the type I transmembrane protein,  $\beta$ -amyloid precursor protein (APP). The formation of this complex may be important for modulation of the processing and function of APP. APP is proteolytically cleaved at multiple sites. The cleavages and their regulation are of central importance in the pathogenesis of dementias of the Alzheimer type. In cell cultures and perhaps *in vivo*, secretion of the  $\alpha$ -cleaved APP ectodomain (sAPP $\alpha$ ) is the major pathway in the most cells. Regulation of the process may require extracellular/intracellular cues. Neither extracellular ligands nor intracellular mediators have been identified, however. Here, we show novel evidence that the major isoform of FE65 (97-kDa FE65, p97FE65) can be converted to a 65-kDa N-terminally truncated C-terminal fragment (p65FE65) via endoproteolysis. The cleavage region locates immediately after an acidic residue cluster but before the three major protein-protein binding domains. The cleavage activity is particularly high in human and non-human primate cells and low in rodent cells; the activity appears to be triggered/enhanced by high cell density, presumably via cell-cell/cell-substrate contact cues. As a result, p65FE65 exhibits extraordinarily high affinity for APP (up to 40-fold higher than p97FE65) and potent suppression (up to 90%) of secretion of sAPP $\alpha$ . Strong p65FE65-APP binding is required for the suppression. The results suggest that p65FE65 may be an intracellular mediator in a signaling cascade regulating  $\alpha$ -secretion of APP, particularly in primates.**

FE65 is a multimodular adaptor protein, consisting of three major protein-protein interaction domains, a WW domain and two phosphotyrosine interaction domains (PID)<sup>1</sup> (1, 2)

(Fig. 2A). The interaction between FE65 and APP mainly takes place between the C-terminal PID (PID2) and the APP intracellular domain (AICD), although other regions may also potentially contribute to the action. The physiological effects of FE65-APP complexes are not well understood. Genetic evidence suggests that strong FE65-APP binding was favored by natural selection during animal evolution toward human lineage (3). APP is a widely studied protein because of its role in the pathogenesis of dementias of the Alzheimer type (DAT). FE65 is predominantly expressed in central nervous system neurons, and its expression is regulated during development and aging, with high levels corresponding to the timing of neural tissue formation and high neuronal activity (4–8). Selective knock-out of the p97FE65 isoform results in modest impairments in learning but severe deficits in relearning spatial tasks (8). These phenotypes reflect reduced synaptic plasticity. Thus, the APP-FE65 pathway may play roles in normal and abnormal cognitive functions.

In addition to binding to AICD, FE65 can also interact, at least *in vitro*, with several other proteins through its WW and PID1 domains (1, 2). FE65 is able to translocate between the nucleus and cytoplasm, consistent with the distinct locations of its multiple binding partners. Through these protein-protein interactions, FE65 may impact upon APP processing (9–12), gene expression (13, 14), pre-mRNA splicing (15), cell cycle progression (16), plasma membrane dynamics (17, 18), axonal projection and neuronal positioning (19), and learning and memory (8).

As a type I transmembrane protein, APP can undergo serial proteolytic processing at sites within or near the transmembrane domain; dysfunction of the process is thought to be the underlying mechanism of DAT (20, 21). APP processing involves at least two consecutive cleavages. Cleavages by  $\alpha$ - or  $\beta$ -secretases release large soluble ectodomains, sAPP $\alpha$  or sAPP $\beta$ , into extracellular environments and leave small C-terminal fragments retained in membranes. These membrane-bound fragments may be further cleaved by  $\gamma$ -secretases leading to release and secretion of non-pathogenic p3 peptides or potentially pathogenic A $\beta$  peptides and AICD (20). Under physiological conditions,  $\alpha$ -cleavage of APP is the major and ubiquitous pathway of APP metabolism in most cells. That cleavage precludes production of A $\beta$  peptides, whereas suppression of  $\alpha$ -cleavage of APP may potentially provide more substrates for  $\beta$ -secretase. The regulation of APP processing is thought to occur at the level of ectodomain shedding via extracellular or intracellular cues (22, 23).

Unlike some other  $\gamma$ -secretase-cleaved transmembrane proteins, the extracellular cues or ligands that are potentially responsible for the regulation of APP secretion have not yet been identified. Secretion of the ectodomains of APP in cell culture seems to occur constitutively (“by default”) (20, 21). On the other hand, several lines of evidence consistently show that

\* This work was supported in part by NIA, National Institutes of Health Research Grants AG19711 (to G. M. M.) and AG05136-19 (a pilot study award to Q. H.). The costs of publication of this article were defrayed in part by the payment of page charges. This article must therefore be hereby marked “advertisement” in accordance with 18 U.S.C. Section 1734 solely to indicate this fact.

<sup>‡</sup> To whom correspondence should be addressed: Dept. of Pathology, Box 357470, University of Washington, Seattle, WA 98195. Tel.: 206-616-4226; Fax: 206-685-8356; E-mail: qhu@u.washington.edu.

<sup>1</sup> The abbreviations used are: PID, phosphotyrosine interaction domain; A $\beta$ ,  $\beta$ -amyloid peptides; AICD, APP intracellular domain; APP,  $\beta$ -amyloid precursor protein; ARC, acidic-residue cluster; CTF, APP C-terminal fragments; DAT, dementias of the Alzheimer type; GST, glutathione S-transferase; LRP, low density lipoprotein receptor-related protein 1; p97FE65, major full-length FE65 isoform; p97FE65a2, minor full-length FE65 isoform generated by alternative splicing; p65FE65, 65-kDa N-terminally truncated C-terminal fragment derived from p97FE65; p65FE65a2, 65-kDa N-terminally truncated C-terminal fragment derived from p97FE65a2; PARP, poly(ADP-ribose) polymerase; PBS, phosphate-buffered saline; sAPP $\alpha$ , secreted  $\alpha$ -cleaved APP ectodomain; HA, hemagglutinin; FITC, fluorescein isothiocyanate.

deletion of the AICD or introduction of mutations into this domain promotes APP secretion (24–27). This suggests that the conserved AICD may normally play a suppressive role. The regulation most likely requires interactions with AICD-binding proteins. Although AICD is rather small (only about 47 amino acid residues in length), it can be bound by more than 12 proteins and/or their family members, at least based upon *in vitro* evidence (2). FE65 is the prototypical AICD-binding protein. Despite direct binding, the impact of FE65 on secretion of APP ectodomains has been somewhat controversial (9–12, 28). This inconsistency may be due to the results having been obtained under various experimental settings; it may also reflect the intrinsic complexity of the FE65 molecule and the cellular environments with which FE65 interacts in different biological contexts. We now demonstrate that p97FE65 can undergo endoproteolysis, leading to production of p65FE65. p65FE65 exhibits extraordinarily high affinity for AICD and strong suppression of secretion of sAPP $\alpha$ . These results suggest a novel cellular mechanism by which secretion of sAPP $\alpha$  is regulated, particularly in primate cells.

#### EXPERIMENTAL PROCEDURES

**Cell Cultures and DNA Transfection**—Cell cultures were performed as described previously (6). For transient transfection, cells were seeded at 80–90% of confluence before transfection. Transfection was mediated by polyethylenimines (Polysciences, Inc., Warrington, PA) as described previously (29). Typically, 1.2  $\mu$ g of total plasmid DNAs and 6  $\mu$ l of polyethylenimines were used for one well of the 12-well plates. Downstream assays were usually performed at 24–48 h after transfection.

**Recombinant Constructs**—All human FE65 constructs were derived from previously described parental constructs (3) or their modifications. Double-tagged *pcDNA3.1-HA-p97fe65-myc* was generated by insertion of a HA tag into the N-terminal FE65 in *pcDNA3.1-p97fe65-myc*. The modified construct was then used for generations of deletions/mutations by site-directed mutagenesis; these were utilized for the mapping of p97FE65 cleavage sites. Various non-tagged FE65 constructs in a *pcDNA3.1* vector were used for the experiments where comparisons with endogenous FE65s were needed or for APP secretion assays. The C-terminal Myc-tagged *pcDNA3.1-fe65-myc* constructs were generated and used for the experiments on immunocytochemical localizations or APP secretion. *pGEX-APPC48*, coding for a fusion protein between glutathione *S*-transferase (GST) and the 48 C-terminal amino acids of the human APP, was from the previous study (3). *pGEX-KG-Tip60* (63–454), coding for a fusion protein between GST and Tip60, was a gift from Dr. Thomas C. Sudhof (the University of Texas Southwestern Medical Center). *pGEX-LRPC101* (4445–4544), coding for a fusion protein between GST and the 101 C-terminal residues of human low density lipoprotein receptor-related protein 1 (LRP), was PCR subcloned from *pcDNA3.1-mLRP4T100*, a gift from Dr. Guojun Bu (Washington University, St. Louis). Constructs of *pCA-APP695*, *pCA-S $\beta$ C*, and *pCA-APP $\Delta$ AICD* were obtained from previous studies (30). All insert sequences were verified by DNA sequencing. A synthetic peptide containing the C-terminal 57 residues of APP (C57) was purchased from rPeptide (Athens, GA).

**Antibodies**—Affinity-purified anti-FE65 polyclonal antibodies FE27 and FE518 were described previously (3, 8). The epitope sequences have no homology to FE65L1 and FE65L2 and are completely conserved between human and mouse. Anti-HA monoclonal 16B12, Alexa-Fluor-594–16B12, anti-Myc monoclonal 9E10 and FITC-labeled 9E10 were purchased from Babco (Richmond, CA); anti-APP-N-terminal monoclonal 22C11 and anti-A $\beta$ <sub>1–17</sub> monoclonal 6E10 were from Chemicon (Temecula, CA); anti- $\beta$ -actin monoclonal and anti-APP-C-terminal polyclonal (for immunostaining) were from Sigma; anti-APP-C-terminal polyclonal (O443) (for Western blotting) was a generous gift from Dr. Kumar Sambamurti (the Mayo Clinic, Jacksonville, Florida) (31); anti-caspase-3 and anti-PARP (poly(ADP-ribose) polymerase) polyclonal were from BD Biosciences; anti-cyclin B1 polyclonal was from Santa Cruz Biotechnology (Santa Cruz, CA).

**Western Analysis and GST Pull-down Binding Assays**—Western analysis was performed as described previously (3, 8). FE65 antibodies were used at 1:20,000 dilutions; commercial antibodies were used at dilutions suggested by the manufacturers, except for antibodies 22C11 and 6E10, which were used at 1:15,000 dilutions. GST pull-down assays were performed as described previously (3). GST-APPC48 pull-down

was performed in a modified binding/lysis buffer (50 mM Tris-HCl, pH 7.5, 150 mM NaCl, 0.5% Triton X-100, 10% glycerol, 50 mM NaF, 1 mM sodium vanadate) supplemented with EDTA-free Complete™ protease inhibitors (Roche Applied Science) prior to use. GST-LRPC101 and GST-Tip60 pull-down were performed in LRP binding/lysis buffer (20 mM Tris-HCl, pH 7.5, 150 mM NaCl, 2 mM CaCl<sub>2</sub>, 2 mM MgCl<sub>2</sub>, 1% Triton X-100) supplemented with the same protease inhibitors. Fresh monkey cerebral cortex lysates (from a 10-year-old female *Macaca nemestrina*) were generous gifts from Dr. John Glomset (the Primate Center, University of Washington). Autopsy human brain tissues (with a post-mortem interval of ~3 h) were from a non-demented 65-year-old female. Mouse brain tissues were from 6-month-old C57BL/6J females. The use of human subjects and animals in the study has complied with all relevant federal guidelines and institutional policies. Brain tissues were homogenized in corresponding binding/lysis buffers and centrifuged at 14,000 rpm at 4 °C for 20 min; supernatants were used for Western analysis or pull-down assays. Statistical analysis was performed by two-tailed Student's *t* test.

**Immunocytochemistry**—COS cells were plated on coverslips in 24-well plates. Immunostaining was conducted 24 h after transfection. Cells were fixed in 3.7% paraformaldehyde/phosphate-buffered saline (PBS) at room temperature for 30 min, permeabilized in 0.15% Triton X-100/PBS at room temperature for 5 min, and blocked in 5% fetal bovine serum/PBS-T (0.2% Tween 20 in PBS) at room temperature for 30 min. For staining APP, cells were incubated with 22C11 or anti-APP-C-terminal polyclonal antibody at 1:500 dilutions in 1% fetal bovine serum/PBS-T at room temperature for 30–60 min. After washes with PBS-T, cells were incubated with an Alexa-Fluor-568-conjugated secondary antibody at 1:200 dilutions (Molecular Probes, Eugene, OR). For staining Myc-tagged FE65s or HA-tagged mLRP4, FITC-9E10 or Alexa-Fluor-594–16B12 was used at 1:200 dilutions. Samples were mounted in a 4',6-diamidino-2-phenylindole medium and visualized by standard immunofluorescence microscopy with the facilities provided by the Keck Center at the University of Washington.

#### RESULTS

**An N-terminally Truncated C-terminal FE65 Fragment Exhibits High Affinity for AICD**—In previous experiments, we observed an ~65-kDa protein fragment that could be pulled down together with p97FE65 by GST-APPC48 and recognized by an FE65-specific antibody FE518 (3). The results suggested that the fragment might be a truncated FE65. To map the fragment, a double-tagged neuronal isoform p97FE65 cDNA was generated (Fig. 2A) and expressed in COS cell cultures. Western analysis revealed that the 65-kDa fragment could be recognized by antibodies specific to C-terminal epitopes (FE518 or Myc) but not by those specific to N-terminal epitopes (HA and FE27) (Fig. 1A), indicating that it contains the distal two-thirds of the C-terminal region of p97FE65. We named the fragment p65FE65.

Endogenous p65FE65 protein bands were also detected in cerebral cortex lysates of freshly prepared monkey brain (Fig. 1B) and in lysates prepared from human and non-human primate confluent cell cultures, including COS cells and a brain neuroblastoma cell line, SK-N-SH (Fig. 1D). Similar results were also observed in HEK cells and brain neuroblastoma cell lines IMR32 and MC65 (data not shown). In contrast, endogenous p65FE65 was rarely detected in lysates of the counterpart tissues/cell cultures from rodents, although these tissues/cells expressed relatively abundant p97FE65 (Fig. 1, B and D). The results suggest that p65FE65 is predominantly produced in primates. The endogenous p65FE65 fragments could also be dramatically enriched by GST-APPC48 pull-down (Fig. 1, C and E, compare with Fig. 1, B and D), as ratios of p65FE65/p97FE65 were increased 10–40-fold after the treatments (Fig. 1F, left). The enrichments were not because of an AICD-induced event because p65FE65/p97FE65 ratios were not changed during incubation with GST-APPC48 (Fig. 1G). These results suggest that p65FE65 has extraordinarily high affinity for AICD. Although Western analysis of lysates prepared from autopsy human cerebral cortexes detected neither p97FE65 nor p65FE65 bands (data not shown), GST-APPC48 pull-down enriched the p65FE65 bands (Fig. 1C).

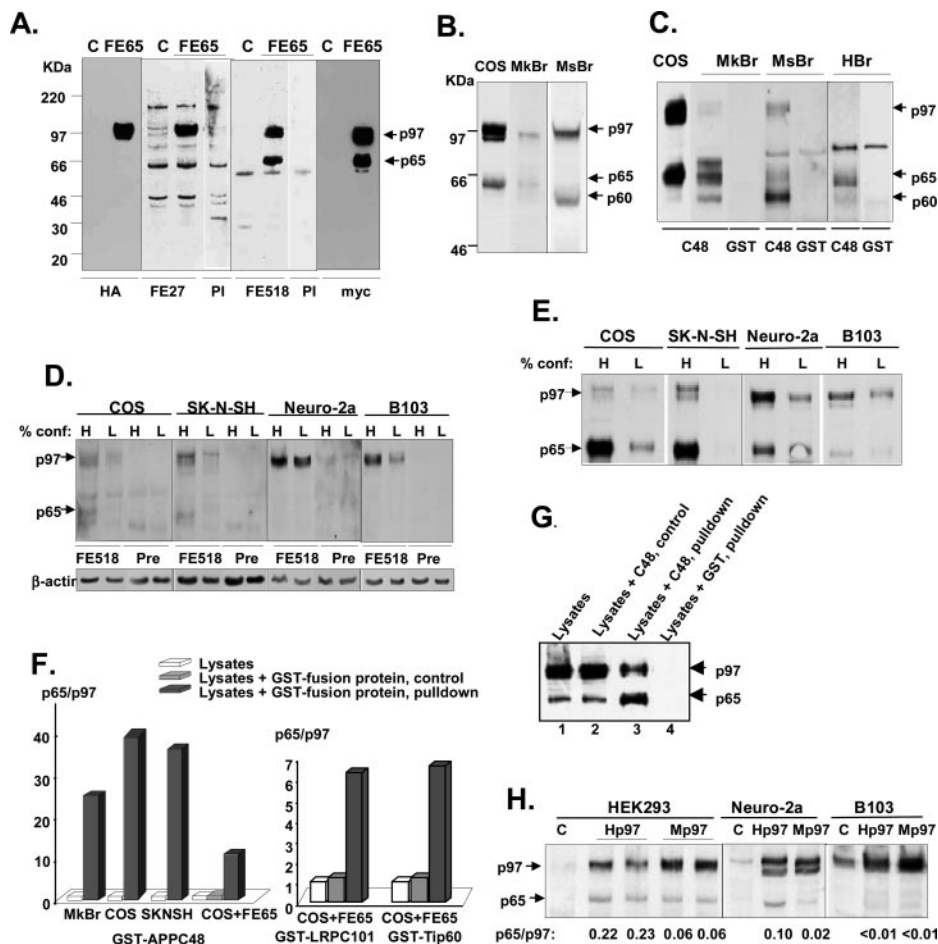


**FIG. 1. An N-terminally truncated C-terminal FE65 fragment (p65FE65) has high affinity for AICD.** A, lysates of COS cell cultures transfected with *pcDNA3.1-HA-p97fe65-myc* were analyzed by Western blotting with antibodies 16B12 (anti-HA), FE27, FE518, or 9E10 (anti-Myc) or the corresponding preimmune serum (PI). p97, p97FE65; p65, p65FE65; C, *pcDNA3.1* vector controls. B and C, lysates freshly prepared from a monkey cerebral cortex (MkBr) or a C57BL/6J mouse cortex (MsBr) were analyzed by Western blotting with antibody FE518 (10  $\mu$ g of protein/lane) (B). COS cell lysates overexpressing p97FE65 were used as references. These brain lysates along with cerebral cortex lysates of a human autopsy brain (HBr) were also analyzed by GST or GST-APPC48 (C48) pull-down (250  $\mu$ g of protein/sample) followed by Western blotting with FE518 (C). D and E, lysates of various cell cultures grown to 25% (L lanes) or 100% (H lanes) confluence (conf) were analyzed by Western analysis (D) or by GST-APPC48 pull-down (E) as described in B and C. Levels of  $\beta$ -actin were used as loading controls. COS, a SV-40-transformed African green monkey kidney cell line; SK-N-SH, Neuro-2a, and B103, brain neuroblastoma cell lines from human, mouse, and rat, respectively; Pre, preabsorbed FE518. Results similar to those of SK-N-SH or COS cells were also observed in human neuroblastoma cell lines IMR32, MC65, and HEK293 (data not shown). F, left panel, p65/p97 ratios of selected samples in B–E were compared before and after subjecting to GST-APPC48 pull-down analysis. Right panel, p65/p97 ratios of COS cell lysates overexpressing p97FE65 were compared before and after being subjected to GST-LRPC101 or GST-Tip60 pull-down analysis. G, COS cell lysates expressing *pcDNA-p97fe65-myc* were incubated with GST-APPC48 (C48) without pull-down (lane 2) or with pull-down (lane 3) followed by Western analysis with anti-Myc antibody. H, HEK293, Neuro-2a, or B103 cells were transfected with human *pcDNA-p97fe65-myc* (Hp97), mouse *pcDNA-p97fe65-myc* (Mp97), or *pcDNA3.1* (C lanes). Lysates were analyzed by Western blotting with FE518.

To examine the interactions of p65FE65 with other binding partners, pull-down assays with GST-LRPC101 (a fusion protein between GST and the 101 C-terminal residues of human LRP) or GST-Tip60 (a fusion protein between GST and Tip60) were also performed. Both LRP and Tip60 have previously been shown to bind the PID1 domain (13, 32). The results revealed that the p65FE65 (but not p97FE65) bands were also enriched by GST-LRPC101 or GST-Tip60 pull-down but not by incubation with these fusion proteins alone (controls) (Fig. 1F, right). A reasonable interpretation is that the N-terminal region of p97FE65 has inhibitory functions for multiple downstream protein-protein interactions; removal of this region is apparently responsible for the great enhancement of these bindings.

A previously described 60-kDa p60FE65 detected in mouse brain tissues (8) was also detected in non-human primates and human brain tissues (Fig. 1, B and C). Although both p60FE65 and p65FE65 are N-terminally truncated C-terminal fragments, p60FE65 is generated by alternative translation downstream of exon 2 and is rarely detected in cell cultures. In

contrast, p65FE65 is generated by endoproteolytic cleavage within a region encoded by exon 2 (see below) and can be detected in confluent cultures. Because p60FE65 lacks part of the WW domain, this isoform may not have the same functional roles as p65FE65 does.<sup>2</sup>

To investigate what caused rodent cells to produce only small amounts of p65FE65, we compared the ratios of p65FE65/p97FE65 in lysates of confluent HEK, Neuro-2a, and B103 cells expressing human or mouse p97FE65 cDNA sequences (Fig. 1H). The results suggest that neither rodent protein sequences nor cell environments favor the production of p65FE65.

**p65FE65 Is a Cleaved Product of p97FE65**—Because p65FE65 is also produced from the cDNA construct coding for p97FE65, it is unlikely to be a product of alternative splicing. Instead, the fragment might be generated via endoproteolytic cleavage of p97FE65 or alternative translation from the

<sup>2</sup> B. H. Cool, Q. Hu, and G. M. Martin, unpublished observations.



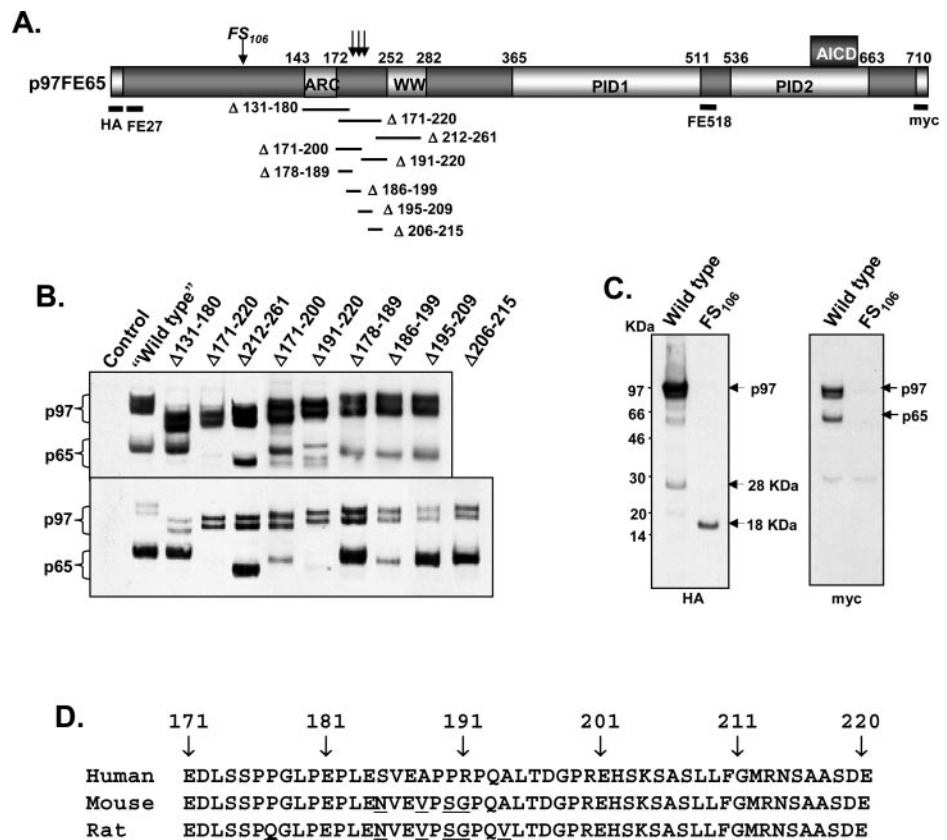


**FIG. 2. p65FE65 is endoproteolytically cleaved from p97FE65.** **A**, a schematic diagram indicates the positions of deletions ( $\Delta$ ) and a frameshift mutation (FS) in HA-p97FE65-Myc ("wild type"). The numbers correspond to the human FE65 amino acid sequences (GenBank<sup>TM</sup> accession number L77864). WW, WW domain; AICD, APP intracellular domain that interacts with FE65 PID2. **B**, generations of p65FE65 in COS lysates expressing the wild-type and mutant constructs were examined by Western analysis (top) with FE518 or by GST-APPC48 pull-down followed by Western analysis (bottom). **C**, expression of a frameshift mutant HA-p97FE65FS<sup>106</sup>. Myc in COS cells prematurely terminated translation of p97FE65 (left panel) and also abolished production of p65FE65 (right panel). **D**, comparisons of the amino acid residues between 171 and 220 among human, mouse, and rat FE65s. The non-conserved residues are underlined.

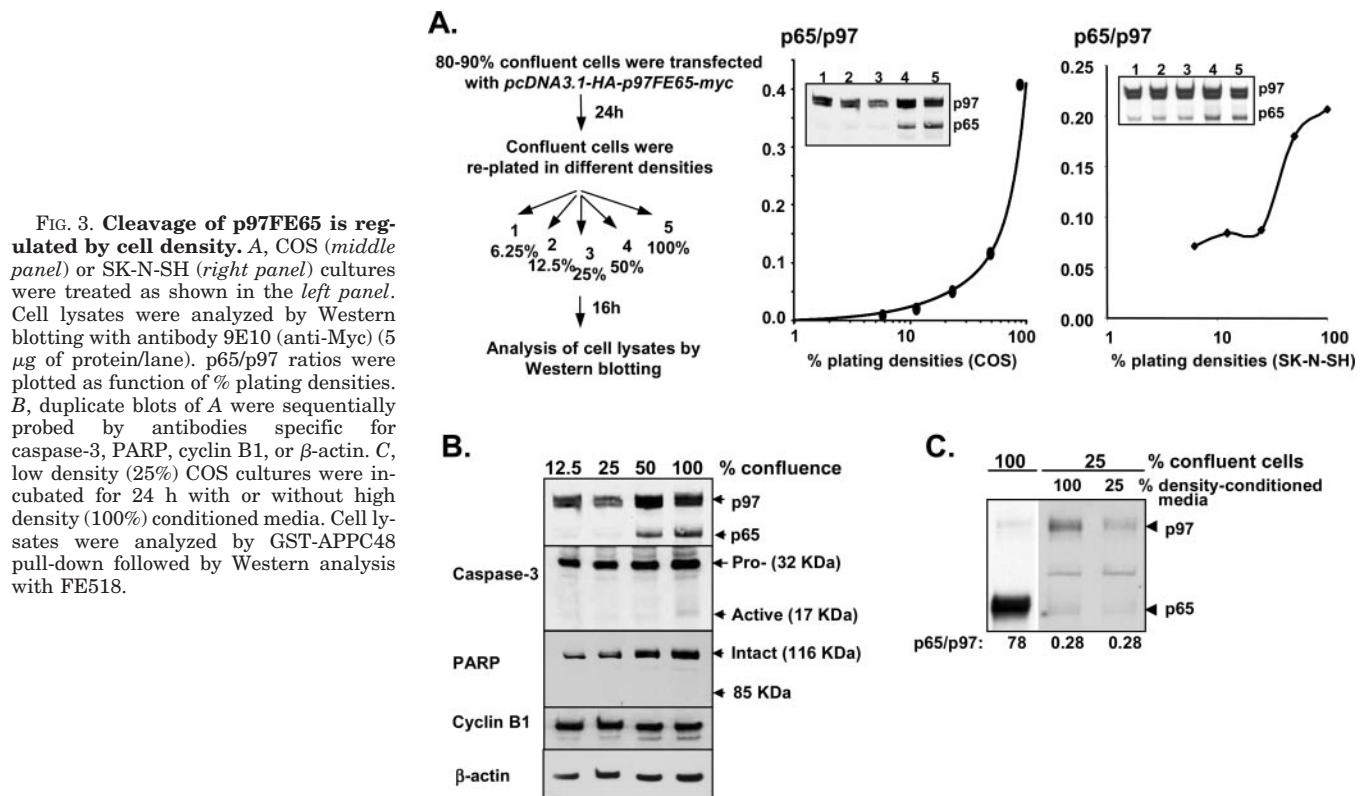
p97FE65 open reading frame. To determine which mechanism is responsible for generation of p65FE65, we mapped the N terminus of p65FE65. Initial efforts at microsequencing of affinity-purified p65FE65 were unsuccessful because of N-terminal blockage. As an alternative approach, deletion ( $\Delta$ ) analysis was performed using a panel of mutant constructs generated from the *pcDNA3.1-HA-p97fe65-myc* (wild type) (Fig. 2A). The results showed that  $\Delta$  (residues) 131–180 reduced the size of the larger band but did not affect the production of p65FE65, whereas  $\Delta$ 212–261 reduced the sizes of both the p65FE65 and p97FE65 bands, suggesting that the N terminus is located downstream of residue 180 but upstream of residue 212 (Fig. 2B). This assumption was confirmed by  $\Delta$ 171–220, which completely abolished the production of p65FE65. A further smaller deletion ( $\Delta$ 191–220 but not  $\Delta$ 171–200) within this region also partially disrupted generation of p65FE65 but resulted in some minor nonspecific bands (Fig. 2B). Interestingly, when deletion regions were smaller than 15 residues ( $\Delta$ 178–189,  $\Delta$ 186–199,  $\Delta$ 195–209, and  $\Delta$ 206–215) within this region, no significant interference occurred (Fig. 2, A and B), suggesting that generation of p65FE65 requires a specific secondary or tertiary structure. Large deletions might disturb the conformation, whereas small ones might not significantly perturb the structure. The results suggest the possibility of heterogeneous proteolytic cleavages at multiple sites within a small region rather than that of alternative translation, which usually involves initiation from a definite codon. A combination analysis of the results of  $\Delta$  131–180,  $\Delta$ 171–220,  $\Delta$ 212–261, and  $\Delta$ 191–220 suggests that the putative cleavage site most likely is located between residues 191 and 212, although  $\Delta$ 171–220 showed the most efficient interruption.

The endoproteolytic cleavage hypothesis was further tested by a frameshift mutation (a single T insertion) introduced to residue 106 (FS<sup>106</sup>) that resulted in the premature termination of p97FE65 translation at residue 118, upstream of the putative cleavage site(s) (Fig. 2A). In addition to the premature

termination of p97FE65, the mutation would also lead to two mutually exclusive outcomes: (a) uninterrupted expression of p65FE65, indicating that p65FE65 was generated by alternative translation from an internal in-frame codon; or (b) abolished expression of p65FE65, confirming that p65FE65 was generated by endoproteolytic cleavage of p97FE65. The results revealed that the frameshift mutation abolished the production of p97FE65 as well as p65FE65 (Fig. 2C, right), producing a single ~18-kDa peptide corresponding to the size of the prematurely terminated N-terminal peptide (Fig. 2C, left). Therefore, we concluded that p65FE65 is derived from p97FE65 via endoproteolytic cleavage. In this particular experiment, we also observed an ~28-kDa fragment corresponding to the size of the cleaved N-terminal product from the wild-type p97FE65 (Fig. 2C, left). The fragment was not often detectable (e.g. Fig. 1A), suggesting that it might be unstable.

A comparative sequence analysis revealed the following. 1) FE65 residues 171–220 are not conserved in FE65L1 and FE65L2, members of the FE65 family. Thus, the endoproteolytic cleavage at this site is a unique feature of FE65 processing. 2) Residues 171–220 are not completely conserved in the FE65 proteins of human, mouse, and rat (Fig. 2D), which may partially explain the inefficient cleavage of p97FE65 in rodent cells. 3) The endoproteolytic cleavage separates a previously uncharacterized acidic residue cluster (ARC) from the downstream major protein-binding domains (Fig. 2A). The ARC (E<sup>143</sup>QGPDEGEKKAAGEAEEEEEDDDDEEEEEED<sup>172</sup>), enriched for polyglutamic acids, is also absent in FE65L1 and FE65L2 but conserved in FE65 of human, mouse, and rat.

We cloned a human p65FE65 starting with a Met codon followed by codons 193–710. The design was based upon: 1) the mutation analyses shown in Fig. 2, A and B; 2) the PeptideCutter analysis (us.expasy.org/tools/peptidecutter) between residues 191 and 212, suggesting an endopeptide cleavage site between residues 192 and 193. Expression of the cloned p65FE65 in COS cells yielded a protein fragment migrating at



a position identical to that of the cleavage product from p97FE65 in SDS-PAGE.

Attempts to identify the class of the protease(s) responsible for the p97FE65 cleavage were unsuccessful. We screened candidate proteases with a protease inhibitor set (Roche Applied Science), including inhibitors specific for metalloproteinases, aspartic proteases, serine and cysteine proteases, and aminopeptidases. Each inhibitor was separately added to the lysates of COS cells expressing p97FE65. Ratios of p65FE65/p97FE65 were not changed as a result of these treatments. The results suggest that the responsible protease(s) may become inactive once cells are lysed.

**Cleavage of p97FE65 May Be Regulated by Cell Density**—The evidence that especially abundant p65FE65 fragments were produced in confluent primate cell cultures raised the possibility that the cleavage activity might be regulated by cell density. To test that possibility, we designed the experiments illustrated in Fig. 3A (left panel). To avoid the up-regulated expression of endogenous p97FE65 at high cell densities confounding the analysis (Fig. 1, D and E), we analyzed exogenous p97FE65 expressed from pcDNA3.1-HA-p97fe65-myc. As shown in Fig. 3A, levels of the exogenous p97FE65 at cell-plating densities between 6.25% (lane 1) and 100% (lane 5) were not much different under these conditions. In contrast, the ratios of p65FE65/p97FE65 were dramatically increased as cell densities increased, reflecting up-regulated p97FE65 cleavage activity. In COS cells, cleavage activity was inactive at low cell density, became active in ~50% confluent cells, and reached peak levels when cultures were 100% confluent (Fig. 3A, middle panel). Similar but less robust results were observed in SK-N-SH cells (Fig. 3A, right panel). These results suggest that high cell density can trigger or enhance the cleavage activity in cultures and presumably *in vivo*, where high density is the norm.

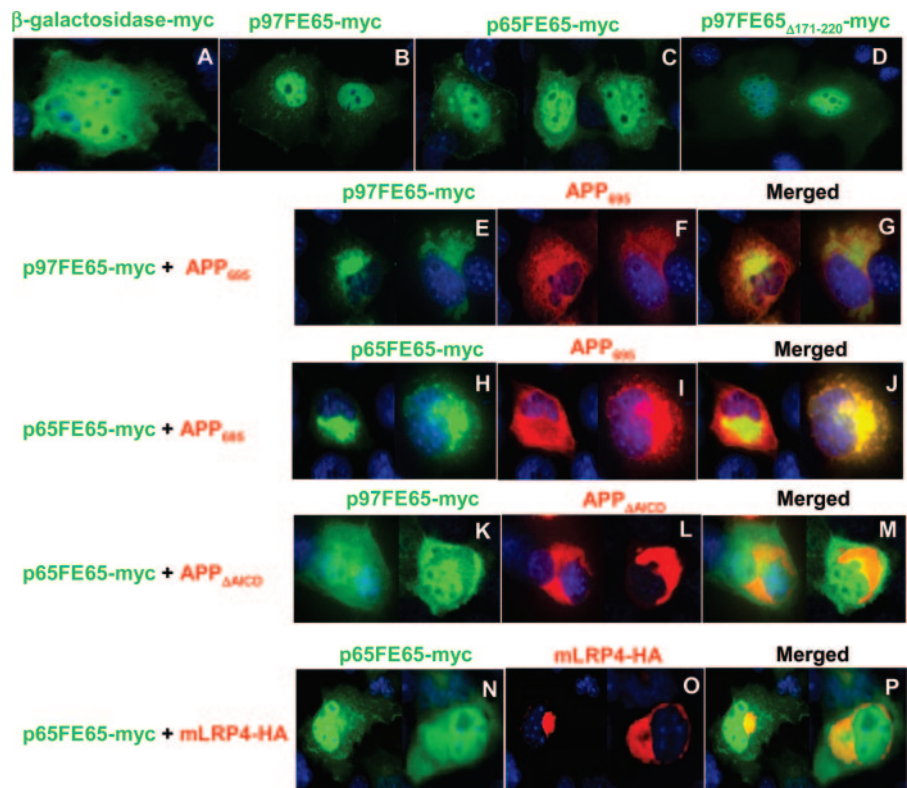
To assess whether cleavage was a consequence of other cellular events, *e.g.* apoptosis and cell cycle arrest, which are often associated with high cell density, we examined COS lysates for the expression of several reference marker proteins, including

caspase-3 (converted from the 32-kDa pro-active form to the 17- and 12-kDa active forms during early/middle apoptosis), PARP (converted from a 116-kDa inactive form into an 85-kDa active form during late apoptosis), and cyclin B1 (a G<sub>2</sub>/M phase cell cycle marker). The results showed that cleavage of p97FE65 occurred earlier than cleavage of caspase-3 or PARP (Fig. 3B) and that the levels of cyclin B1 were not changed during the experimental period. The results suggest that cleavage of p97FE65 is not the consequence of apoptosis, and it appears to be independent of cell cycle alterations.

To determine what factors, soluble or insoluble, were involved in the regulation, low density COS cell cultures were treated with high density conditioned media. The ratios of p65FE65/p97FE65 were not changed by that treatment (Fig. 3C), suggesting that soluble factors may not contribute to the regulation; instead, the regulation is likely mediated by cell-cell or cell-substrate contacts. This interpretation is consistent with the negative results of the protease inhibitor experiments (above). The cleavage may be active only when the appropriate contact cues are present.

**Cellular Locations of p97FE65 and p65FE65 Are Modulated by APP but Not by LRP**—To assess whether the enhanced affinity of p65FE65 for APP and LRP could affect the cellular locations of p65FE65, immunostaining was performed in COS cells transfected with various constructs (Fig. 4). In the absence of co-transfections with APP, the major immunoreactivities of p97FE65, p97FE65 $\Delta$ 171–220, and p65FE65 were in the nucleus (Fig. 4, A–D), with relatively more p65FE65 immunoreactivity found in perinuclear structures or on plasmic membranes (Fig. 4C). These findings suggest that under endogenous APP concentrations, p65FE65 may be more readily tethered in the cytoplasm than the uncleaved proteins, perhaps because of its high affinity for APP (13, 33). In contrast, co-transfections with APP resulted in the tethering of all FE65 proteins in perinuclear structures (presumably Golgi/endoplasmic reticulum) independently of strong or weak APP binding (Fig. 4, E–J). The action requires AICD, as APP $\Delta$ AICD (in which

**FIG. 4. Cellular locations of p97FE65 and p65FE65 are regulated by APP but not by LRP.** A–D, COS cells transfected with plasmids coding for the indicated Myc-tagged proteins and fixed cells were immunostained with FITC-9E10. E–J, COS cells were co-transfected with *pCA-APP695* and *pcDNA3.1-p97fe65-myc* or *pcDNA3.1-p65fe65-myc* and then co-stained with FITC-9E10 (green) and an anti-AICD antibody (red). K–M, COS cells were co-transfected with *pCA-APP $\Delta$ AICD* (APP695 with the  $\gamma$ -cleaved C-terminal fragment deleted and replaced by 59 residues derived from the 3'-untranslated region sequences of APP695) and *pcDNA3.1-p65fe65-myc* and were co-stained with FITC-9E10 (green) and antibody 22C11 (red). N–P, COS cells were co-transfected with *pcDNA3-mLRP4T100-HA* (coding for the membrane-containing minireceptor of LRP, mLRP4-HA) and *pcDNA3.1-p65fe65-myc* and were co-stained with FITC-9E10 (green) and Alexa-Fluor-594–16B12 (anti-HA) (red). Nuclei were stained blue with 4',6-diamidino-2-phenylindole.



the C-terminal 59 residues of APP695 was deleted and replaced by novel 59 residues translated from the APP695 3'-untranslated region) lacked such effects (Fig. 4, K–M). To our surprise, unlike APP, mLRP4-HA (the membrane-containing minireceptor of LRP) (34) was unable to tether either p97FE65 (data not shown) or p65FE65 (Fig. 4, N–P) in the cytoplasm, although mLRP4-HA also accumulated in the same perinuclear structures. These results suggest that APP has a unique function for regulation of FE65 cellular localizations. The observations raise the possibility that the presence of certain threshold amounts of APP may be prerequisites for cytoplasmic functions that require LRP-FE65 binding.

**p65FE65 Is a Potent Suppressor of the Secretion of sAPP $\alpha$** —To investigate whether cleavage of p97FE65 could impact APP processing and function, we compared the effects of cleaved and uncleaved FE65 (Fig. 5A) on secretion of sAPP $\alpha$  in multiple cell lines. As shown in Fig. 5B, co-expression of p65FE65 and human APP695 in HEK293 cells significantly reduced levels of sAPP $\alpha$  in conditioned media and the ratios of sAPP $\alpha$ /cellular APP by 90%, when compared with mock transfections (co-transfections of the *pcDNA3.1* vector and APP695). The effects were p65FE65 dose-dependent (Fig. 5C). In contrast, overexpression of p97FE65 $\Delta$ 171–220 or p97FE65 modestly reduced secretion of sAPP $\alpha$  by 25–60% (Fig. 5, B and C), which is consistent with the observations by Ando *et al.* (9). The results indicate that p65FE65 is a strong suppressor of the secretion of sAPP $\alpha$ , although uncleaved p97FE65 may also have weak suppressive functions in this cell line.

To determine whether tight FE65-AICD binding is essential for the suppression, APP695 was also co-transfected with p97FE65a2 or its cleaved derivative, p65FE65a2. As described previously (3), the p97FE65a2 isoform is expressed in all rodents and non-human primates as well as in ~25% of Northern European populations because of the presence of a minor FE65 allele that causes alternative splicing of exon 14. However, rodents, non-human primates, and carriers of the minor allele also express various amounts of the “normal” splicing isoform,

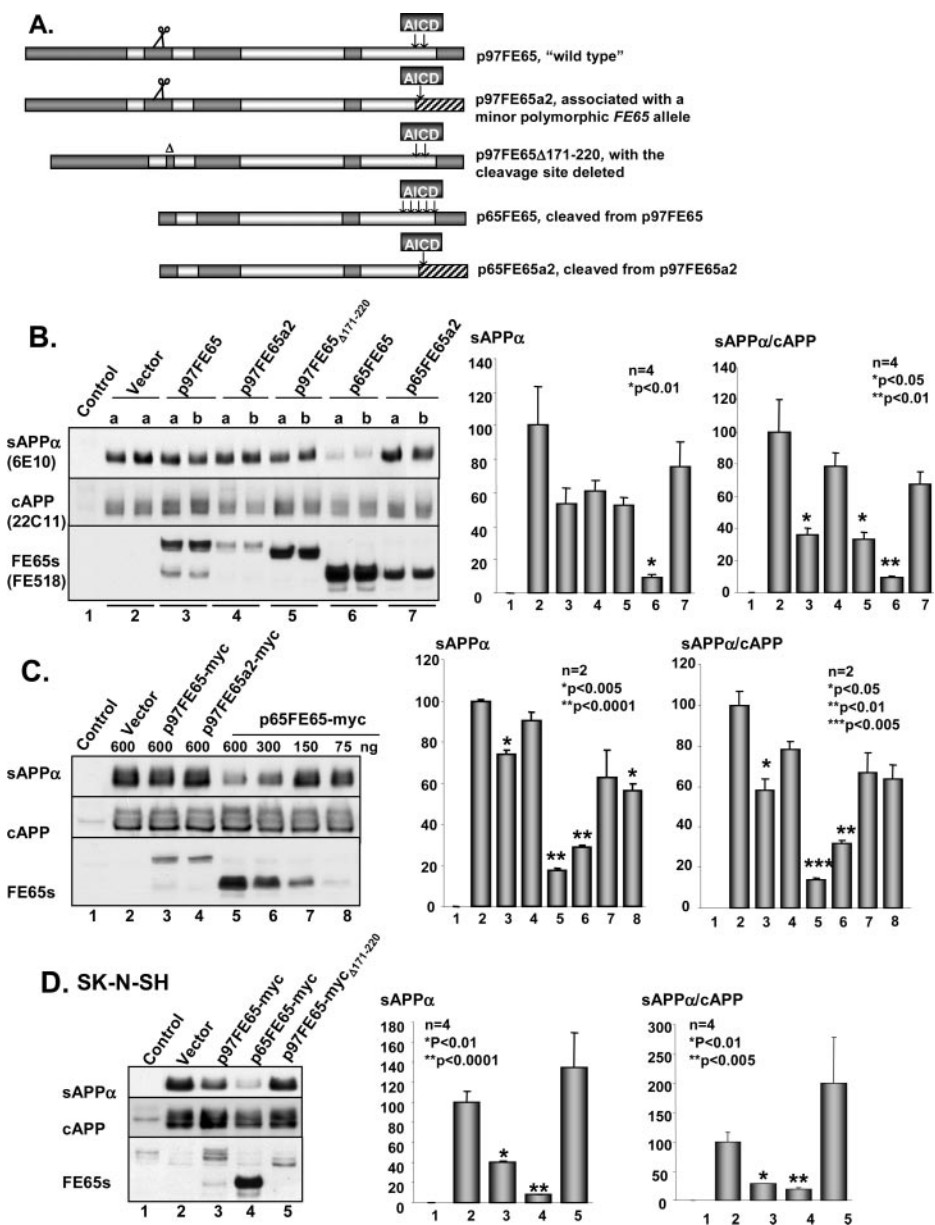
p97FE65. p97FE65 and p97FE65a2 are similar in size but have different C-terminal regions leading to high and low APP binding affinity, respectively (3) (Fig. 5A). Remarkably, p97FE65a2 and p65FE65a2 showed no effects on secretion of sAPP $\alpha$  by either measurement (Fig. 5B), although both proteins could be efficiently tethered in the perinuclear structures by co-transfected APP in COS cells (data not shown). The results indicate that strong FE65-APP interaction is essential for the suppressive action.

To demonstrate the generality of our observations, we tested several other cell lines. In SK-N-SH cell cultures, p65FE65 or p97FE65 also exhibited potent or modest suppressions of sAPP $\alpha$  secretion, by 80–90 and 60–70%, respectively, whereas the uncleaved p97FE65 $\Delta$ 171–220 had no such effects (Fig. 5D). In COS, Neuro-2a, and B103 cells, however, only p65FE65 significantly suppressed secretion of sAPP $\alpha$  (by 60–70%), whereas p97FE65, p97FE65 $\Delta$ 171–220, and p97FE65a2 had no such effects (Fig. 5, E–G). In general, strong suppressions were observed in human cell lines, moderate suppressions were seen in a non-human primate cell line, and there was weak suppression in rodent cell lines. Consistent with these results, knockdown of FE65 levels by short interference RNA showed increased secretion of APP (12). In addition, the effects of cell density on secretion of endogenous sAPP $\alpha$  were evaluated in HEK293 cells (Fig. 5H). The results showed that secretion of sAPP $\alpha$  was inversely regulated by cell density.

We should point out that the actual suppressive effects might be larger than observed because immunostaining results revealed that 80–90% of co-transfected cells showed strong staining of both FE65 and APP; the other 10–20% showed strong staining of either APP or FE65 (data not shown), suggesting that secretion of sAPP $\alpha$  in those cells mainly overexpressing APP might have escaped the regulation by FE65. Secondly, the expression levels of p65FE65 were always stronger than those of any other FE65 isoforms/fragments (Fig. 5, B–G). This was not because of the variations of transfection efficiencies, as the differences were persistent after normalization of FE65 levels to



**FIG. 5. p65FE65 shows potent and dose-dependent suppression of secretion of sAPP $\alpha$ .** A, a schematic diagram shows FE65 isoforms/fragments. Number of arrows indicates their relative affinities for AICD. B, HEK293 cells were co-transfected with *pCA-APP695*, *pcDNA3.1-LacZ*, and the indicated FE65 construct. Two independent clones (referred to as *a* and *b*) of each *fe65* construct were used to eliminate potential artifacts due to cloning and plasmid preparation. Conditioned media and cell lysates were analyzed by Western blotting with antibodies 6E10 and 22C11 or FE518, respectively. Loading was normalized to relative activities of  $\beta$ -galactosidase. Values are presented as mean  $\pm$  S.E. Control, no transfection. C, p65FE65 shows dose-dependent suppression of secretion of sAPP $\alpha$ . HEK293 cells were co-transfected with equal amounts of *pCA-APP695* and various amounts of *fe65* constructs. Total amounts of plasmid DNA/well (12-well plates) were made up to 1.2  $\mu$ g with the *pcDNA3.1* vector. Samples were analyzed as described in B. D–G, SK-N-SH, COS, Neuro-2a, and B103 cells were co-transfected with *pCA-APP695* and the indicated *fe65* constructs. Samples were analyzed as described in B. H, effects of cell densities on  $\alpha$ -secretion of endogenous APP. HEK293 cells were maintained at the indicated cell densities for 20 h; conditioned media or cell lysates were analyzed by Western blotting with antibody 6E10 or 22C11 ( $n = 4$ ). Sample loading was normalized to cell numbers. C, unconditioned culture medium. I, effects of FE65s on levels of APP C-terminal fragments. HEK293 cells were co-transfected with *pCA-APP695*, *pcDNA3.1-LacZ*, and the indicated *fe65* constructs. Cell lysates or conditioned media were analyzed by Western blotting with antibody O443 as described previously (31) or with 6E10 ( $n = 2$ ). Sample loading was normalized to relative activities of  $\beta$ -galactosidase. Control, no transfection; C99, the *pCA-S $\beta$ C* vector consisting of the signal sequence of APP fused to its C-terminal 99 residues was transfected into HEK293 cells for use as standards for  $\beta$ / $\alpha$ CTF; C57, a synthetic peptide containing the C-terminal 57 residues of APP was used as a standard for  $\gamma$ CTF.



$\beta$ -galactosidase activity controls. Similarly, globally stronger immunostaining was also evident in cells expressing p65FE65 than those expressing any other FE65 forms (data not shown). These observations suggest that p65FE65 may be more stable than other FE65 forms. Thirdly, using sensitive enzyme-linked immunosorbent assays (35), we were unable to detect reliable levels of the  $A\beta_{40}$  and  $A\beta_{42}$  peptides in conditioned media (with or without supplement of serum) under these experimental conditions (the  $R$  values of typical standard curves were 0.9754–0.9967 when concentrations of the  $A\beta_{40}$  or  $A\beta_{42}$  standard peptides were between 31.25–1000 pg/ml), suggesting that the levels of the  $A\beta$  peptides in our samples may be below 31.25 pg/ml.

To evaluate the influences of various FE65 forms on the levels of APP C-terminal fragments (CTFs), we examined the CTF profiles of HEK293 cells co-expressing APP695 and various FE65s (Fig. 5I). Consistent with the results of the  $A\beta$  enzyme-linked immunosorbent assays,  $\gamma$ CTF bands were undetectable. However, we detected strong peptide bands corresponding to the positions of  $\alpha$ CTF. In general, the  $\alpha$ CTF profiles were consistent with those of sAPP $\alpha$  (i.e. high levels of sAPP $\alpha$  corresponding to relative high levels of  $\alpha$ CTF) with a few exceptions. For example,

cells with the mock transfections (control) secreted the highest levels of sAPP $\alpha$  but did not express the highest levels of  $\alpha$ CTF. This may be due to the fact that the CTFs can be stabilized by forming complexes with FE65 (36). Without co-transfection with FE65, degradation of  $\alpha$ CTF in the control samples may be faster than those of the samples in which FE65 was co-transfected. In addition, although the lowest levels of  $\alpha$ CTF were also detected in p65FE65-co-transfected cells, the magnitudes of reduced  $\alpha$ CTF were smaller than those of the reduced secretion of sAPP $\alpha$ . The differences may reflect the dual effects of p65FE65 on  $\alpha$ CTF, with p65FE65 reducing secretion of sAPP $\alpha$  (presumably leading to reduced  $\alpha$ CTF levels) as well as stabilizing  $\alpha$ CTF (resulting in increased levels of  $\alpha$ CTF). The faint peptide bands above  $\alpha$ CTF apparently corresponded to  $\beta$ CTF. As levels of these bands were low and varied slightly between Western analyses of the same samples, quantitative analysis of these bands was not performed.

#### DISCUSSION

**p97FE65 Is Cleaved by Regulated Protease Activity**—In this study, we demonstrate that p97FE65 can undergo endoproteolytic cleavage, generating p65FE65 and a small unstable N-

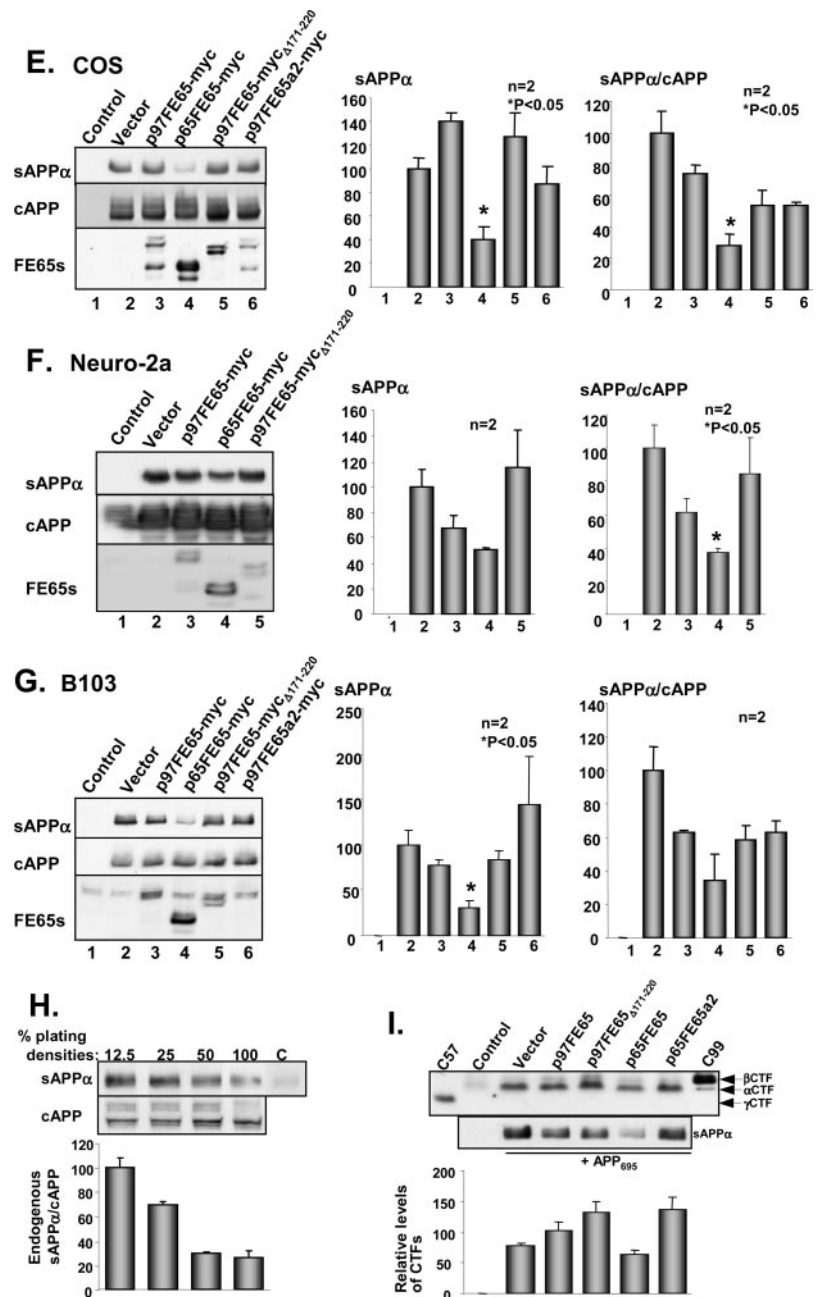


FIG. 5—continued

terminal fragment. The cleavage activity is more active in cells/brain tissues derived from primates than those found in the counterpart cells/tissues of rodents. By deletion analysis, the major cleavage site is mapped between residues 191 and 212. However, the cleavage may occur in a rather flexible fashion within a range of fewer than 50 residues between residues 171 and 220 (Fig. 2). This is characteristic of some proteolytic enzymes (37, 38). These cleavages may be influenced by physical length or secondary and tertiary structural characteristics of the cleavage domain. Deletion of residues 171–220 sufficiently disrupts the putative structure along with all potential cleavage sites. It remains to be determined which proteases are involved and where the cleavage occurs at the subcellular level.

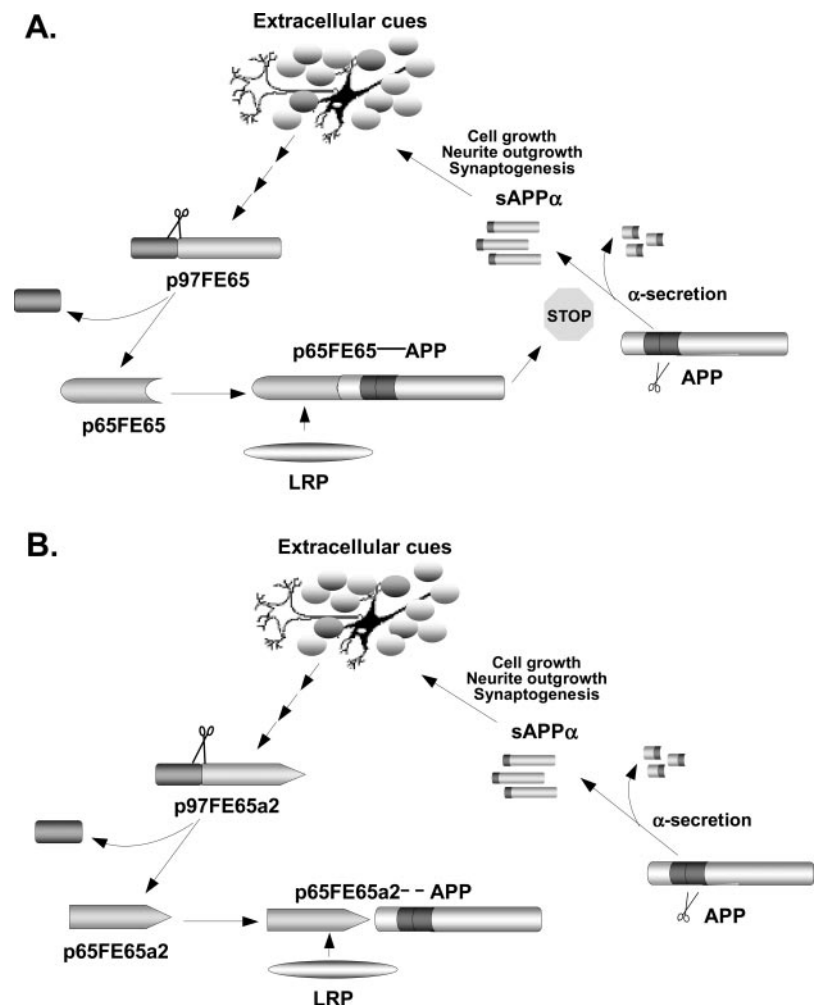
Despite the promiscuous sequence specificity, p97FE65 cleavage activity is regulated. The cleavage activity appears to be triggered (e.g. in COS cells) or enhanced (e.g. in SK-N-SH cells) by relatively high cell density. The regulation is apparently independent of apoptotic and cell cycle signals, and it is not medi-

ated by soluble factors. One potential interpretation is that extracellular contact cues (cell-cell or cell-substrate contact) are involved. FE65 and APP have been shown to co-localize at mobile membranes and growth cones (17, 18). Molecules in these structures may easily sense contact-mediated cues for guiding them to their appropriate targets (39). FE65 may be one of those molecules that is sensitive to suitable contact cues and able to convert such cues into intracellular signals. This notion is also consistent with evidence that sAPP functions in neurite outgrowth, synaptogenesis, synaptic plasticity, and cell-cell adhesion (21, 40). These cellular activities apparently require appropriate cell-cell or cell-substrate communications.

*Is p97FE65 a Pro-protein?*—The cleavage sites on p97FE65 are located immediately after the ARC but before the major protein-protein binding domains. The unique position suggests that the cleavage may remove a region with regulatory influences on downstream protein-protein interactions. Consistent with this proposition, we found that alterations of certain properties are associated with removal of the N terminus. First,



**FIG. 6. A putative feedback pathway regulating sAPP $\alpha$  secretion by FE65.** A, sAPP $\alpha$  is constitutively secreted into extracellular environments in low density cell cultures. When cell cultures become confluent, extracellular cues trigger/enhance the putative protease activity and convert p97FE65 to a potent suppressor of secretion of sAPP $\alpha$  via strong p65FE65-APP binding. The feedback route may persist unless new cues are established. B, in contrast, weak p65FE65a2-APP binding lacks such suppression. The feedback loop may therefore be absent or ineffectual (see "Discussion" for details).



removal of this region profoundly enhances formations of APP-p65FE65, LRP-p65FE65, and Tip60-p65FE65 complexes *in vitro*. Second, removal of the region appears to stabilize p65FE65. The increased protein stability may be a consequence of the enhanced protein-protein binding, as proteins in protein complexes are perhaps less accessible by proteases. The enhanced affinity and stability may have synergic effects on downstream cellular events, *e.g.* suppression of secretion of sAPP $\alpha$ .

However, p97FE65 may not serve only as a pro-protein. The ARC closely resembles clusters found in nuclear chaperones. These domains mediate molecular interactions, particularly between proteins (*e.g.* histones) and nucleic acids during DNA replication and transcription (41). It remains possible that p97FE65 and p65FE65 assemble different molecular complexes in the nucleus, as both proteins can translocate into that compartment. Given the nuclear chaperone-like ARC in p97FE65 and the enhanced interactions between Tip60-p65FE65, we compared the transactivation activities of p97FE65 and p65FE65 using an APP-Gal4 reporter system, which had been used previously to demonstrate a requirement of FE65 for AICD nuclear signaling (13). The results revealed that p65FE65 slightly reduced transactivation activities (by 15–45%) when compared with p97FE65. Because the assay system relies on cleavages of APP, interpretations of the relative small differences can be potentially confounded by many events, including APP processing, nuclear translocation, and protein-protein interactions. These events can simultaneously but differentially influence the performances of p97FE65 and p65FE65 in the assay. Thus, novel assays need to be developed

for the assessment of the functions of p97FE65 and p65FE65 in the nucleus. Recent evidence also indicates that the ARC in p97FE65 might have special affinity for calcium ions (42). However, the physiological relevance of these *in vitro* experiments is unclear.

**p65FE65 May Be an Intracellular Mediator of the sAPP $\alpha$  Pathway in Primates**—We show that the p97FE65 cleavage event may be involved in the regulation of the sAPP $\alpha$  pathway. Cleavage of p97FE65 produces a strong suppressor of the secretion of sAPP $\alpha$ , presumably via the tight binding of p65FE65 to AICD. This may partially explain why strong FE65-APP binding had been selected during animal evolution. We have shown previously that the major *fe65* polymorphic allele that only produces p97FE65 has been selected in human (3). This is in contrast to the minor human allele, which is more closely aligned with non-human *fe65* sequences, producing both p97FE65 and p97FE65a2 (3). Here, we also show that the p97FE65 cleavage activity and its potential modifiers (presumably encoded by loci other than *fe65*) that lead to robust AICD binding are also very active in primates. These events together may lead to particularly robust and regulated p65FE65-AICD interactions in our species. Interestingly, carriers of the minor *fe65* allele are relatively resistant to very late onset DAT (3, 43, 44). Failures to confirm these findings in other case control studies may be related to the age structures of the study populations (3). Tight p65FE65-AICD binding may suppress secretion of sAPP $\alpha$  by one of several non-mutually exclusive mechanisms. 1) Tight p65FE65 binding may directly alter the conformation of the distal regions of APP, making the latter an unfavorable substrate for  $\alpha$ -secretases. 2) Enhanced affinities

of p65FE65 for multiple binding partners may lead to increased p65FE65 stability. 3) Increased affinity of p65FE65 for LRP may recruit LRP to the site of AICD, as formation of LRP-FE65-APP trimeric complexes may be part of the mechanism for down-regulation of the secretion of APP (12). It is not clear whether the modulation by p65FE65 occurs on the cell surface or during transport in secretory vesicles. Immunostaining (Fig. 4) indicates that majorities of p65FE65 and APP remain together in secretory vesicles, however. In addition, recent evidence suggests that the cleavages of APP can occur at normal rates without APP ever reaching the cell surface but largely requires that APP traverse the Golgi complex (45).

Our results help to resolve controversial reports about the impacts of FE65 on APP secretion. Sabo *et al.* (11) showed that overexpression of a rat *fe65* cDNA in Madin-Darby canine kidney cells increased secretion of sAPP $\alpha$ . The overexpressed 97-kDa FE65 proteins were apparently uncleaved in those cells, which, therefore, might mimic the effects of the uncleaved p97FE65 $\Delta$ 171–220, producing increased secretion of sAPP $\alpha$  in some cell lines (Fig. 5). Overexpression of human FE65L1 in the human neuroglioma cell line H4 or of FE65L2 in HEK293 cells showed an increased impact or no impact on secretion of sAPP $\alpha$  (10, 28). Because the two family members share only 40–50% amino acid similarities with FE65 and also lack the cleavage region we discovered in this study, they might either resemble the effects of the uncleaved p97FE65 $\Delta$ 171–220 or influence APP processing by different mechanisms.

Our findings may lead to a novel mechanism by which cleavage of p97FE65 and generation of p65FE65 may be prerequisites for the efficient modulation of the sAPP $\alpha$  pathway. The putative mechanism is apparently very effective in primates. Identification of the receptors/ligands responsible for the regulation of APP-ectodomain secretions has been elusive. Recently, the secreted glycoprotein F-spondin has been shown to bind the APP ectodomain and to suppress products of  $\alpha$ - and  $\beta$ -secretases, but the physiological relevance of this observation is still unclear (46). Deletions of some portions of the APP ectodomain do not disturb its secretion,<sup>3</sup> suggesting that the regulation of APP secretion may be through the AICD, mediated by AICD binding factors. Several AICD-binding proteins have exhibited such potential. Co-expressions of X11 or the c-Jun N-terminal kinase-interacting protein JIP1b with APP suppress secretion of sAPP $\alpha$  or sAPP $\alpha$ / $\beta$  (26, 47). Mutations of the YENPTY motif in AICD, which is responsible for binding by X11, JIP1b, and FE65, result in increased secretion of sAPP $\alpha$  (26). In addition, reduction of APP secretion by LRP requires FE65-binding motifs located in the LRP cytoplasmic domain (12, 48). However, connections of these regulations to extracellular cues have not been established. We now show that only cleaved p65FE65 exhibits potent suppressive effects; the cleavage appears to be triggered/enhanced by high cell densities, presumably via cell-cell or cell-substrate contact cues. FE65, therefore, may be one of the key adaptors to provide links between extracellular environments to the APP tail. The discovery of the FE65 cleavage site may provide a novel therapeutic target for optimizing the processing of APP.

**A Putative Feedback System for Modulation of APP  $\alpha$ -Secretion**—The suppression of APP  $\alpha$ -secretion by cleaved FE65 is consistent with a negative feedback model as outlined in Fig. 6. In subconfluent cell cultures, sAPP $\alpha$  is constitutively secreted into culture media. When cell cultures become confluent, cells somehow sense altered contact cues and activate an intracellular signaling cascade leading to p97FE65 cleavage. Removal of the unstable N terminus of p97FE65 leads to remarkably

increased affinity for APP, probably through altered conformation of the C-terminal binding domains. These events ultimately lead to potent suppression of the secretion of sAPP $\alpha$  (Fig. 6A). Enhanced binding affinities may also allow p65FE65 to recruit other binding partners, such as LRP, to the site of the APP tail for these actions. The feedback route may persist unless new contact cues are established, such as when cells are replated at low density. Although p97FE65a2 can also undergo the proteolytic cleavage, the cleaved product is unable to contribute to the regulation pathway because of inefficient binding of APP; the feedback loop is thus disconnected (Fig. 6B).

How might these putative mechanisms work in the adult brain? One can imagine that in the brain, cells and extracellular matrix have been densely packed in all dimensions, which could, potentially, consistently activate the putative cleavage protease. Alternatively, the cleavage activity may be sensitive to special contact cues at micro-environmental settings, such as where neurite outgrowth or synaptic remodeling is taking place. The model is consistent with the evidence that the FE65 and APP families may have overlapping functions in axonal projection and neuronal positioning during development (19, 49–51). Because the p97FE65 cleavage is more active in the cells and tissues from non-human primates and humans than in those from rodents, the feedback pathway may represent one of a number of “fine-tuning” mechanisms that have been adapted to more sophisticated functions in these high species. For example, processing and metabolism of APP in rodents differ from those of humans. Human-APP transgenic mice, for example, never develop the same neuropathology seen in DAT brains (52). Creation of a high fidelity model of DAT in laboratory mice may therefore require the “humanization” of many loci related to APP metabolism, including its many binding partners.

**Acknowledgements**—We thank Dr. Thomas C. Sudhof for the *pGEX-KG-Tip60(63–454)* construct, Dr. Guojun Bu for the *pcDNA3.1-mLRP4T100* construct, Dr. John A. Glomset for monkey brain lysates, Dr. Lee-way Jin for autopsy human brain tissues, and Dr. Kumar Sambamurti for antibody O443.

## REFERENCES

- Russo, T., Faraonio, R., Minopoli, G., De Candia, P., De Renzis, S., and Zambrano, N. (1998) *FEBS Lett.* **434**, 1–7
- King, G. D., and Turner, R. S. (2004) *Exp. Neurol.* **185**, 208–219
- Hu, Q., Cool, B. H., Wang, B., Hearn, M. G., and Martin, G. M. (2002) *Hum. Mol. Genet.* **11**, 465–475
- Simeone, A., Duilio, A., Fiore, F., Acampora, D., De Felice, C., Faraonio, R., Paolocci, F., Cimino, F., and Russo, T. (1994) *Dev. Neurosci.* **16**, 53–60
- Bressler, S. L., Gray, M. D., Sopher, B. L., Hu, Q., Hearn, M. G., Pham, D. G., Dinulos, M. B., Fukuchi, K., Sisodia, S. S., Miller, M. A., Distèche, C. M., and Martin, G. M. (1996) *Hum. Mol. Genet.* **5**, 1589–1598
- Hu, Q., Hearn, M. G., Jin, L. W., Bressler, S. L., and Martin, G. M. (1999) *J. Neurosci. Res.* **58**, 632–640
- Kesavapany, S., Banner, S. J., Lau, K. F., Shaw, C. E., Miller, C. C., Cooper, J. D., and McLoughlin, D. M. (2002) *Neuroscience* **115**, 951–960
- Wang, B., Hu, Q., Hearn, M. G., Shimizu, K., Ware, C. B., Liggitt, D. H., Jin, L. W., Cool, B. H., Storm, D. R., and Martin, G. M. (2004) *J. Neurosci. Res.* **75**, 12–24
- Ando, K., Iijima, K. I., Elliott, J. I., Kirino, Y., and Suzuki, T. (2001) *J. Biol. Chem.* **276**, 40353–40361
- Guenette, S. Y., Chen, J., Ferland, A., Haass, C., Capell, A., and Tanzi, R. E. (1999) *J. Neurochem.* **73**, 985–993
- Sabo, S. L., Lanier, L. M., Ikin, A. F., Khorkova, O., Sahasrabudhe, S., Greengard, P., and Buxbaum, J. D. (1999) *J. Biol. Chem.* **274**, 7952–7957
- Pietrzik, C. U., Yoon, I. S., Jaeger, S., Busse, T., Weggen, S., and Koo, E. H. (2004) *J. Neurosci.* **24**, 4259–4265
- Cao, X., and Sudhof, T. C. (2001) *Science* **293**, 115–120
- Baek, S. H., Ohgi, K. A., Rose, D. W., Koo, E. H., Glass, C. K., and Rosenfeld, M. G. (2002) *Cell* **110**, 55–67
- Muresan, Z., and Muresan, V. (2004) *Hum. Mol. Genet.* **13**, 475–488
- Bruni, P., Minopoli, G., Brancaccio, T., Napolitano, M., Faraonio, R., Zambrano, N., Hansen, U., and Russo, T. (2002) *J. Biol. Chem.* **277**, 35481–35488
- Sabo, S. L., Ikin, A. F., Buxbaum, J. D., and Greengard, P. (2001) *J. Cell Biol.* **153**, 1403–1414
- Sabo, S. L., Ikin, A. F., Buxbaum, J. D., and Greengard, P. (2003) *J. Neurosci.* **23**, 5407–5415
- Guenette, S. Y., Chang, Y., Hiesberger, T., Richardson, J. A., and Herz, J. (2003) *Soc. Neurosci. Abstr.* (Abstr. 336.10)

<sup>3</sup> Z. Yang, Q. Hu, and G. M. Martin, unpublished observations.

20. Selkoe, D. J. (2001) *Physiol. Rev.* **81**, 741–766
21. Annaert, W., and De Strooper, B. (2002) *Annu. Rev. Cell Dev. Biol.* **18**, 25–51
22. Monning, U., Sandbrink, R., Weidemann, A., Banati, R. B., Masters, C. L., and Beyreuther, K. (1995) *J. Biol. Chem.* **270**, 7104–7110
23. Kopan, R., and Ilangan, M. X. (2004) *Nat. Rev. Mol. Cell. Biol.* **5**, 499–504
24. Haass, C., Hung, A. Y., Schlossmacher, M. G., Teplow, D. B., and Selkoe, D. J. (1993) *J. Biol. Chem.* **268**, 3021–3024
25. Kouchi, Z., Kinouchi, T., Sorimachi, H., Ishiura, S., and Suzuki, K. (1998) *Eur. J. Biochem.* **258**, 291–300
26. Sastre, M., Turner, R. S., and Levy, E. (1998) *J. Biol. Chem.* **273**, 22351–22357
27. Tomita, S., Kirino, Y., and Suzuki, T. (1998) *J. Biol. Chem.* **273**, 19304–19310
28. Tanahashi, H., and Tabira, T. (2002) *Biochem. J.* **367**, 687–695
29. Thomas, M., and Klivanov, A. M. (2002) *Proc. Natl. Acad. Sci. U. S. A.* **99**, 14640–14645
30. Fukuchi, K., Deeb, S. S., Kamino, K., Ogburn, C. E., Snow, A. D., Sekiguchi, R. T., Wight, T. N., Piussan, H., and Martin, G. M. (1992) *J. Neurochem.* **58**, 1863–1873
31. Pinnix, I., Musunuru, U., Tun, H., Sridharan, A., Golde, T., Eckman, C., Ziani-Cherif, C., Onstead, L., and Sambamurti, K. (2001) *J. Biol. Chem.* **276**, 481–487
32. Trommsdorff, M., Borg, J. P., Margolis, B., and Herz, J. (1998) *J. Biol. Chem.* **273**, 33556–33560
33. Minopoli, G., de Candia, P., Bonetti, A., Faraonio, R., Zambrano, N., and Russo, T. (2001) *J. Biol. Chem.* **276**, 6545–6550
34. Obermoeller, L. M., Chen, Z., Schwartz, A. L., and Bu, G. (1998) *J. Biol. Chem.* **273**, 22374–22381
35. Shie, F. S., Jin, L. W., Cook, D. G., Leverenz, J. B., and LeBoeuf, R. C. (2002) *Neuroreport* **13**, 455–459
36. Kimberly, W. T., Zheng, J. B., Guenette, S. Y., and Selkoe, D. J. (2001) *J. Biol. Chem.* **276**, 40288–40292
37. Migaki, G. I., Kahn, J., and Kishimoto, T. K. (1995) *J. Exp. Med.* **182**, 549–557
38. Sisodia, S. S. (1992) *Proc. Natl. Acad. Sci. U. S. A.* **89**, 6075–6079
39. Huber, A. B., Kolodkin, A. L., Ginty, D. D., and Cloutier, J. F. (2003) *Annu. Rev. Neurosci.* **26**, 509–563
40. Mattson, M. P. (1997) *Physiol. Rev.* **77**, 1081–1132
41. Philpott, A., Krude, T., and Laskey, R. A. (2000) *Semin. Cell Dev. Biol.*, **11**, 7–14
42. Longo, O., Lamberti, A., Zambrano, N., and Arcari, P. (2003) *Biosci. Biotechnol. Biochem.* **67**, 2048–2050
43. Hu, Q., Kukull, W. A., Bressler, S. L., Gray, M. D., Cam, J. A., Larson, E. B., Martin, G. M., and Deeb, S. S. (1998) *Hum. Genet.* **103**, 295–303
44. Lambert, J. C., Mann, D., Goumidi, L., Harris, J., Pasquier, F., Frigard, B., Cotel, D., Lendon, C., Iwatsubo, T., Amouyel, P., and Chartier-Harlin, M. C. (2000) *Neurosci. Lett.* **293**, 29–32
45. Khvotchev, M., and Sudhof, T. C. (2004) *J. Biol. Chem.* **279**, 47101–47108
46. Ho, A., and Sudhof, T. C. (2004) *Proc. Natl. Acad. Sci. U. S. A.* **101**, 2548–2553
47. Taru, H., Kirino, Y., and Suzuki, T. (2002) *J. Biol. Chem.* **277**, 27567–27574
48. Pietrzik, C. U., Busse, T., Merriam, D. E., Weggen, S., and Koo, E. H. (2002) *EMBO J.* **21**, 5691–5700
49. Magara, F., Muller, U., Li, Z. W., Lipp, H. P., Weissmann, C., Staglar, M., and Wolfer, D. P. (1999) *Proc. Natl. Acad. Sci. U. S. A.* **96**, 4656–4661
50. Muller, U., Cristina, N., Li, Z. W., Wolfer, D. P., Lipp, H. P., Rulicke, T., Brandner, S., Aguzzi, A., and Weissmann, C. (1994) *Cell* **79**, 755–765
51. Herms, J., Anliker, B., Heber, S., Ring, S., Fuhrmann, M., and Kretschmar, H., Sisodia, S., and Müller, U. (2004) *EMBO J.* **23**, 4106–4115
52. Schwab, C., Hosokawa, M., and McGeer, P. L. (2004) *Exp. Neurol.* **188**, 52–64